With the clean He^3 beam, alpha spectra were taken at 35°, 25°, and 15° in the laboratory system. The 15° spectrum is shown in Fig. 2. In addition to the alpha group from the $C^{12}(He^3,\alpha)C^{11}$ reaction leading to the first excited state of C^{11}, two closely-spaced groups of alpha particles were observed. The energy shift of the two groups with angle was consistent with the assignment of these two groups to the reaction $O^{16}(He^3,\alpha)O^{15}$, but because of the small permitted change in angle the $N^{15}(He^3,\alpha)N^{14}$ and $O^{17}(He^3,\alpha)O^{16}$ reactions could not be excluded by this measurement. However, the intensity ratio of the two alpha groups from the two different oxygen targets was the same, implying that both alpha groups were due to reaction products of oxygen isotopes. Ascribing the observed alpha groups to the $O^{16}(He^3,\alpha)O^{15}$ reaction, the cross section at 15° in the laboratory system is 0.5 ± 0.2 mb/steradian for the stronger group and 0.06 ± 0.02 mb/steradian for the weaker one. On the other hand, if the observed groups are ascribed to the $O^{17}(He^3,\alpha)O^{16}$ reaction, a cross section of the order of 1 b/steradian is required. Since so large a cross section is very improbable for (He^3,α) reaction at these energies, the identification of these groups as leading to excited states of O^{15} seems established.

The magnetic spectrometer was calibrated by the observation of elastically scattered protons of known energy, and the excitations of the two excited states in O^{15} were found to be 5.195 ± 0.01 Mev and 5.247 ± 0.01 Mev assuming the 4.923-Mev Q-value[1] for the $O^{16}(He^3,\alpha)O^{15}$ ground state. These values are to be compared with 5.276 and 5.305 Mev in N^{15}. The separations are 52 ± 5 kev in O^{15} and 29 kev in N^{15}. Because of the possibility of fairly large level shifts, further work will be necessary to identify corresponding members of the pairs of levels. In addition the excitation of the first excited state of C^{11} was found to be 1.990 ± 0.01 Mev using the same method of calibration.

These results are in agreement with recently reported $O^{16}(He^3,\alpha)O^{15}$ work carried out by the Harwell group.[12]

ACKNOWLEDGMENTS

The author would like to thank Professor C. A. Barnes, Professor R. F. Christy, Professor W. A. Fowler, Professor C. C. Lauritsen, Professor T. Lauritsen, Professor W. Whaling, Dr. R. W. Kavanagh, and Dr. V. Soergel for many valuable suggestions and discussions. The grant from the "J. Stefan" Institute, Ljubljana, is gratefully acknowledged.

[12] K. Allen (private communication).

PHYSICAL REVIEW VOLUME 114, NUMBER 4 MAY 15, 1959

Collective and Interparticle Interactions in Even-Even Nuclei*

B. JAMES RAZ†
Argonne National Laboratory, Lemont, Illinois

(Received August 14, 1957; revised manuscript received January 22, 1959)

A calculation using two equivalent $f_{7/2}$ particles and adding surface effects to the two-body interaction is reported. The effects of increasing the strength of (*a*) the surface interaction and (*b*) the two-particle interaction are computed. The qualitative regularities observed in even-even nuclei in the so-called vibrational region are obtained and the agreement is somewhat better than that with the pure vibrational model. In contrast to earlier calcaulations, these results can give a spin of 2^+ for the second excited state, as often observed. The calculated ratio of $B(E2;2'\rightarrow 2)$ to $B(E2;2\rightarrow 0)$ is less than 1.0. The appropriate values of the deformation parameters x are less than 1.0.

I. INTRODUCTION

As more experimental information is obtained, the regularities observed in even-even nuclei are becoming more obvious. In the region $150<A<185$ and $A>225$, these regularities are the especially simple ones characteristic of rotational spectra,[1] and are explained with great accuracy by the Bohr-Mottelson strong-coupling collective model.[2,3] In order to examine the collective behavior which is also exhibited by even-even nuclei outside these two regions,[4–7] the weak-coupling

* Work performed under the auspices of the U. S. Atomic Energy Commission.

† Present address: Department of Physics, State University, College on Long Island, Oyster Bay, New York.

[1] A. Bohr, *Rotational States of Atomic Nuclei* (E. Munksgaard, Copenhagen, 1954).

[2] A. Bohr and B. R. Mottelson, Kgl. Danske Videnskab. Selskab, Mat.-fys. Medd. **27**, No. 16 (1953).

[3] A. Bohr, Kgl. Danske Videnskab. Selskab, Mat.-fys. Medd. **26**, No. 14 (1952).

[4] G. Scharff-Goldhaber and J. Weneser, Phys. Rev. **98**, 212 (1955).

[5] An excellent survey of the experimental situation and of the theoretical results in the "near harmonic" or "vibrational" region is given by G. Scharff-Goldhaber, Proceedings of the University of Pittsburgh Conference, June 6–8, 1957 (unpublished), pp. 447–479, 506–507.

[6] C. A. Mallmann, *Proceedings of the Second Unuted Nations International Conference on the Peaceful Uses of Atomic Energy, Geneva*, 1958 (United Nations, Geneva, 1958), paper No. 1971, and private communications.

[7] D. M. Van Patter, Bull. Am. Phys. Soc. Ser. II, **3**, 212 and 360 (1958); J. Franklin Inst. **226**, 411 (1958), and private communications.

solutions of the Bohr-Mottelson collective model[2] have been examined.[4,5] This calculation looks promising in over-all characteristics and well worth investigating in more detail.[8] This is the object of the present work.

II. REVIEW OF PREVIOUS WORK AND PRESENT CALCULATIONS

A review of much of the experimental information on even-even nuclei and the associated theoretical work with weak coupling is contained in the review article by Alder, Bohr, Huus, Mottelson, and Winther.[9] The original theoretical analysis of "vibrational" spectra[4] assumed that the surface interaction that leads to collective effects was much smaller than the direct internucleon interactions. The resulting spectrum was essentially a true vibrational one, based on the four-particle state with $J=0$, and the two-particle interaction did not affect the calculation appreciably. Recently, the assumption has been made that the two-particle forces may be considered infinite by comparison to the collective effects, which results in a pure vibrational spectra.[9,10] However, Ford and Levinson,[11] who also examined the effects of weak and intermediate coupling, conclude that interparticle forces are small compared to surface effects for this type of calculation and therefore are not included in their work. The present results show that none of the above assumptions are necessary to fit the experimental results.

The approach in this paper is to examine the results when a weak or intermediate surface interaction is added to the typical two-particle interaction. The effects of increasing (a) the strength of the surface interaction and (b) the strength of the two-particle interaction are computed. The energy levels, wave functions and interesting γ-ray transition rates were calculated using the explicit configuration $(7/2)^2$ with $J=0$, 2, 4, and 6, and the two-body interaction found suitable[12] for Ca^{43}. This calculation included surface interaction to account for the collective effects but neglected configuration interaction, which is found[12,13] to be very small in Cl^{38}, K^{40}, and Ca^{43}. While the calculations are for a specific nucleus, the general features are instructive and the qualitative results probably are typical and will be applied generally, even outside the $f_{7/2}$ shell, in this paper.

The results of the theoretical calculations show that for small deformation, i..e, $x \lesssim 0.7$, the two-particle interaction plays a vital role in determining the spectrum. For almost all choices of the parameters, the spectrum has features like a pure vibrational one. In detail, the results are as follows:

(1) The ground state is always 0^+.

(2) The first excited state is always 2^+.

(3) The second excited state is almost always composed of a level of spin 2^+ and another of spin 4^+ in a close doublet, lying at about twice the energy of the first excited state.

(4) The second 0^+ level lies higher in energy than the second excited state.

(5) For a quite reasonable strength of the two-body interaction,

(a) the second 2^+ level lies below the 4^+ level for $x \lesssim 0.7$;

(b) the first excited state shows qualitatively the same decrease in energy with increasing values of $B(E2; 0 \rightarrow 2)$ as is observed in experiments;

(c) the reduced γ-ray transition probability, $B(E2)$, is much larger for the direct transitions, $2' \rightarrow 2$ and $2 \rightarrow 0$, than for the cross-over transition, $2' \rightarrow 0$ (where 0 denotes the ground state, 2, the first excited state, and 2', the second state with spin 2);

(d) the $M1/E2$ transition rate, $T(M1)/T(E2)$, is less than one for the $2' \rightarrow 2$ transition for typical values of Z, E_γ, and A, both for two protons and two neutrons in the $f_{7/2}$ shell;

(e) the values of $B(E2; 2' \rightarrow 2)/B(E2; 2 \rightarrow 0)$ vary from 0 to a maximum of about 1, as contrasted with a value of 2 predicted by the pure vibrational picture.[5]

Thus, the calculations indicate that many of the qualitative regularities observed in even-even nuclei in the vibrational region can be obtained with an appropriate choice of two-body interaction coupled with a small amount of surface interaction. The agreement is better than that obtained with a pure vibrational spectrum and resolves the problem of having 2^+ for the spin of the second excited state. Measurements of $B(E2; 2' \rightarrow 2)/B(E2; 2 \rightarrow 0)$ would indicate which calculations are in agreement with experiment, since the results of this work give values less than one for this ratio, while the vibrational picture gives a value of two.[5] Sufficient experimental evidence is not yet available on these transition rates.[6,7]

III. DETAILED DESCRIPTION OF PRESENT CALCULATIONS

A more detailed description of the calculations follows, including a description of the nuclear Hamiltonian, the basis wave functions, and the evaluation of the matrix elements of this Hamiltonian. The Hamiltonian can be divided into (a) the shell-model part, $\bar{H}$,

[8] A preliminary report of the present results has been given by the author, Bull. Am. Phys. Soc. Ser. II, **3**, 224 (1958). An explanation for these regularities has also been proposed in terms of a Bohr-Mottelson strong coupling model with "γ-unstable potential." See L. Wilets and M. Jean, Phys. Rev. **102**, 788 (1956). An interesting modification and extension of that work has also appeared. The energy levels and transition rates of an asymmetric top model of the nucleus were computed as a function of γ by A. S. Davydov and G. F. Filippov, Nuclear Phys. **8**, 237 (1958).

[9] Alder, Bohr, Huus, Mottelson, and Winther, Revs. Modern Phys. **28**, 432 (1956).

[10] G. M. Temmer and N. P. Heydenburg, Phys. Rev. **104**, 976 (1956); see also P. H. Stelson and F. K. McGowan, Phys. Rev. **110**, 489 (1958).

[11] K. W. Ford and C. Levinson, Phys. Rev. **100**, 1 (1955).

[12] J. B. French and B. J. Raz, Phys. Rev. **104**, 1411 (1956).

[13] S. P. Pandya and J. B. French, Ann. phys. **2**, 166 (1957).

and (b) the surface-interaction part, H_s. The system treated is that of two equivalent $f_{7/2}$ particles coupled with phonons, quanta of surface excitation.

Since we are using equivalent particles and radial wave functions of harmonic-oscillator type, the form of the two-body interaction alone determines the energy levels for $\bar{H}$ (i.e., for this problem $\bar{H}=$ constant $=H_{12}$). The two-body interaction,[12]

$$H_{12}/\hbar\omega=3D[3-\boldsymbol{\sigma}_1\cdot\boldsymbol{\sigma}_2]\exp(-r^2/r_0^2),$$
$$\text{with } r_0\sim 2.7\times10^{-13}\text{ cm}, \quad (1)$$

which was found suitable for Ca^{43}, was used here. Any two-body interaction which results in the same splitting for the two-particle levels will give the same results. This was a convenient choice for H_{12} but has little significance as far as the final results are concerned. This is given in units of $\hbar\omega$, the basic energy unit of surface oscillation. The value of D suitable for Ca^{43} is $D\hbar\omega=1$ Mev. The techniques and formulas are standard[12] for the evaluation of H_{12}.

The surface-interaction part of the Hamiltonian, and the techniques which are used for its evaluation, are treated thoroughly by Ford and Levinson[11] so that the details are omitted here. Briefly,

$$H_s/\hbar\omega=\tfrac{5}{2}+\textstyle\sum_\mu b_\mu^* b_\mu-(\hbar\omega 2C)^{-\frac{1}{2}}\sum_{i=1}^{N}k(r_i)(G_i+G_i^\dagger), \quad (2)$$

where (1) b_μ^* and b_μ are the creation and destruction operators for phonons of spin S (where $S=2$), and $S_Z=\mu$; (2) $k(r_i)$ is the radial function for the ith nucleon that determines the strength of the coupling; (3) $\hbar\omega$ is the energy of a phonon; (4) C is the surface-deformation parameter in the surface potential energy; (5) $G_i^\dagger$ is the Hermitean conjugate of G_i; and (6) $G_i\equiv\sum_\mu b_\mu Y_{2\mu}(\theta_i,\phi_i)$, where $Y_{2\mu}(\theta_i,\phi_i)$ is the normalized spherical harmonic of the angular coordinates of the ith particle.

It is convenient to follow Bohr and Mottelson[2] and introduce the variable

$$x=k(5/16\pi j\hbar\omega C)^{\frac{1}{2}},$$

where $k=\langle|k_i|\rangle$. This variable, x, can be compared with the variable, K, used by Goldhaber and Weneser[4]:

$$x\hbar\omega=(K/0.67)(5/8\pi j)^{\frac{1}{2}}$$

or, for $j=\frac{7}{2}$ and $\hbar\omega=0.75$ (the value used by Goldhaber and Weneser[4]), $x=0.47K$.

Since we are using symmetric phonon wave functions and antisymmetric nucleon wave functions, the equation

$$\langle|\sum_{i=1}^{N}k(r_i)(G_i+G_i^\dagger)|\rangle=N\langle|k(r_N)(G_N+G_N^\dagger)|\rangle \quad (3)$$

is valid. Also $\sum_\mu b_\mu^* b_\mu$ is equal to P, the number of phonons in the state. The constant $\frac{5}{2}$ is of no importance in this calculation and is omitted. Thus H_s can be written as

$$\langle|H_s|\rangle/\hbar\omega=P-N(8\pi j/5)^{\frac{1}{2}}x\langle|(G_N+G_N^\dagger)|\rangle. \quad (4)$$

The basis wave functions used are $|JRP(I)\rangle$ in which two nucleons of spin $\frac{7}{2}$ are coupled to give a spin of **J**; P phonons of spin 2 are coupled to give a spin of **R**; and then **J** and **R** are coupled to give a total spin of **I**. The nucleon part of the wave functions is antisymmetric under interchange of nucleons, and the phonon part is symmetric under interchange of phonons.

The matrix elements of G_N, and thus of H_s, are easily evaluated. They are

$$\langle JRP(I)|G_N|J'R'P'(I)\rangle=(-1)^{J+R'-I}W(JRJ'R';I2)\cdots\times\langle J\|Y_2(N)\|J'\rangle\langle PR\|b\|P'R'\rangle, \quad (5)$$

where the reduced matrix elements designated by the double bar are defined by Racah.[14] The value of $\langle j'\|Y_2(N)\|j\rangle$ for one nucleon[15] is found from

$$\langle l'\tfrac{1}{2}j'\|Y_2\|l\tfrac{1}{2}j\rangle=(-1)^{\frac{1}{2}-j'}[(2j+1)(2j'+1)/4\pi]^{\frac{1}{2}}C_{\frac{1}{2},-\frac{1}{2}}^{jj'2}, \quad (6)$$

where the $C_{\frac{1}{2},-\frac{1}{2}}^{jj'2}$ are tabulated by de-Shalit.[16] Formulas (8), (10), and (11) in reference 11 gives N times the value of this quantity for more than one nucleon. The value of $\langle\|b\|\rangle$ is obtained from

$$\langle PR\|b\|P'R'\rangle=\delta_{P',P-1}(-1)^{R'-R}[P(2R+1)]^{\frac{1}{2}}\times\langle P-1\,R'|PR\rangle, \quad (7)$$

where the $\langle P-1\,R'|PR\rangle$ are the coefficients of fractional parentage (to be called CFP's) for symmetric phonon wave functions. These CFP's are identical with the space-symmetric orbital CFP's for $l=2$,

$$\langle(d)^{P-1}L'|(d)^PL\rangle(L'=R',L=R),$$

which were tabulated by Jahn[17] for $P\leq4$. The phase is arbitrary and is chosen here to agree with Choudhury[18] and Jahn.[17] The values of $\langle PR\|b\|P-1\,R'\rangle$ are tabulated in Table I. Note that in reference 11 the phase factor $(-1)^{R'-R}$ is not included in the definition of $\langle\|b\|\rangle$.

The matrix elements of $G^\dagger$ are immediately evaluated since

$$\langle JRP(I)|G_N^\dagger|J'R'P'(I)\rangle=\langle J'R'P'(I)|G_N|JRP(I)\rangle.$$

The matrix elements of the Hamiltonian were evaluated, and the Hamiltonian matrices for $I=0$, 2, 4, 6 were diagonalized by the Applied Mathematics Division, Argonne National Laboratory. This was done for the variables $x=0$ to $x=4$, $D=0.2$; $x=0$ to 1.5, $D=1.0$; and $D=0$ to $D=4$, $x=1.0$. Since the computers available cannot handle a matrix larger than 20×20, these calculations could extend only up to a maximum of three phonons of surface excitation for $I=2$, 4, 6.

[14] G. Racah, Phys. Rev. **62**, 438 (1942).
[15] J. B. French, lecture notes, University of Rochester, 1954 (unpublished). See also reference 11 and A. R. Edmonds, *Angular Momentum in Quantum Mechanics* (Princeton University Press, Princeton, 1957).
[16] A. de-Shalit, Phys. Rev. **91**, 1479 (1953).
[17] H. A. Jahn, Proc. Roy. Soc. (London) **A205**, 192 (1951).
[18] D. C. Choudhury, Kgl. Danske Videnskab. Selskab, Mat.-fys. Medd. **28**, No. 4 (1954).

Even then a few of the small terms had to be omitted. To check the validity of this cutoff at three phonons, the matrix for $I=0$ was diagonalized both for a maximum of three phonons and for a maximum of four phonons.

The lowest two eigenvectors for the matrices with $I=0$ and $I=2$ were also computed, and these were used to calculate $B(E2)$ for the γ-ray transitions $2\rightarrow 0$, $2'\rightarrow 0$, and $2'\rightarrow 2$; and also $T(M1)$ for the $2'\rightarrow 2$ transition.

The formula for $B(E2)$, which is easily obtained from the definitions in reference 2, is

$$B(E2)=\frac{1}{2I_i+1}|\langle I_i\|M(2)\|I_f\rangle|^2=\left|\frac{\langle I_i|M(20)|I_f\rangle}{C_{M_f0M_i}{}^{I_f2I_i}}\right|^2, \quad (8)$$

and if only collective effects are considered,

$$\langle I_i|M(20)|I_f\rangle$$
$$=\frac{3ZeR_0^2}{4\pi}\left(\frac{\hbar\omega}{2C}\right)^{\frac{1}{2}}\Big[C_{M_f0M_i}{}^{I_f2I_i}\sum_{JRPR'P'}K(I_i;JRP)$$
$$\times K(I_f,JR'P')(-1)^{J-R-I_f}(2I_f+1)^{\frac{1}{2}}$$
$$\times W(RI_iR'I_f;J2)\langle PR\|b\|P'R'\rangle\Big]$$
$$+\text{the same expression with } (I_iRP\rightleftarrows I_fR'P'), \quad (9)$$

where $K(I,JRP)$ is that amplitude of the wave function for which $\mathbf{J}+\mathbf{R}=\mathbf{I}$ and $\mathbf{R}$ is formed by P phonons.

A similar formula can be obtained for $B(M1)$ (see, for example, reference 2):

$$B(M1)=|\langle I_i|M(10)|I_f\rangle/C_{M_f0M_i}{}^{I_f1I_i}|^2, \quad (10)$$

where $M(10)$ is the operator defined as

$$M(10)=(3/4\pi)^{\frac{1}{2}}\mu_0[g_R\mathbf{R}+\textstyle\sum_i g_s\mathbf{s}^i+\sum_i g_l\mathbf{l}^i], \quad (11)$$

TABLE I. Double-barred reduced matrix elements for the destruction operator of a phonon, b_μ. In this table $|RP\rangle$ stands for the symmetric wave function of P phonons coupled to give a total spin R.

R	P	R'	P'	$\langle RP\|b\|R'P'\rangle$	R	P	R'	P'	$\langle RP\|b\|R'P'\rangle$
0	0	2	1	$(5)^{\frac{1}{2}}$	2	3	4	4	$9(2/7)^{\frac{1}{2}}$
2	1	0	2	$(2)^{\frac{1}{2}}$			4′	4′	0
		2	2	$(10)^{\frac{1}{2}}$	3	3	2	4	$(10/3)^{\frac{1}{2}}$
		4	2	$3(2)^{\frac{1}{2}}$			2′	4′	$-(55/6)^{\frac{1}{2}}$
0	2	2	3	$(7)^{\frac{1}{2}}$			4	4	$-2(3)^{-\frac{1}{2}}$
2	2	0	3	$(3)^{\frac{1}{2}}$			4′	4′	$-2(143/30)^{\frac{1}{2}}$
		2	3	$2(5/7)^{\frac{1}{2}}$			5	4	$(231/10)^{\frac{1}{2}}$
		3	3	$-(15)^{\frac{1}{2}}$	4	3	2	4	$(22/7)^{\frac{1}{2}}$
		4	3	$3(11/7)^{\frac{1}{2}}$			2′	4′	$(7/2)^{\frac{1}{2}}$
4	2	2	3	$6(7)^{-\frac{1}{2}}$			4	4	$2(5/7)^{\frac{1}{2}}$
		3	3	$(6)^{\frac{1}{2}}$			4′	4′	$-2(91/22)^{\frac{1}{2}}$
		4	3	$3(10/7)^{\frac{1}{2}}$			5	4	$-3(7/6)^{\frac{1}{2}}$
		6	3	$(39)^{\frac{1}{2}}$			6	4	$(390/11)^{\frac{1}{2}}$
0	3	2	4	$2(6)^{-\frac{1}{2}}$	6	3	4	4	$2(13/6)^{\frac{1}{2}}$
		2′	4′	$2(11/6)^{\frac{1}{2}}$			4′	4′	$8(165)^{-\frac{1}{2}}$
2	3	0	4	2			5	4	$2(13/5)^{\frac{1}{2}}$
		2	4	$3(10/7)^{\frac{1}{2}}$			6	4	$(182/11)^{\frac{1}{2}}$
		2′	4′	0			8	4	$(68)^{\frac{1}{2}}$

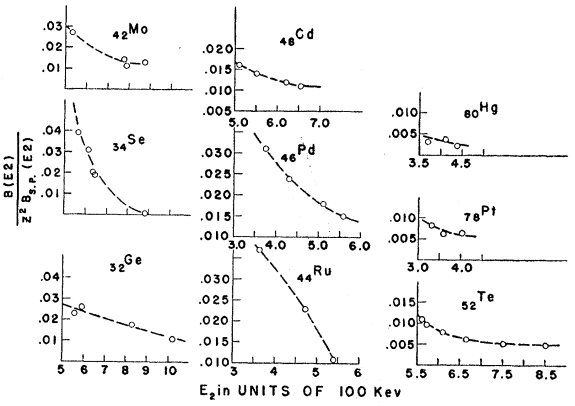

FIG. 1. Experimental values of $B(E2)/Z^2B_{SP}(E2)$ for the transition from $0^+\rightarrow 2^+$ in even-even nuclei *vs* the energy E_2 of the first excited state. The quantity $B_{SP}(E2)$ is the value corresponding to the prediction of the single-particle shell model and is set equal to $e^2\times 3\times 10^{-5}A^{4/3}\times 10^{-48}$ cm^4, the dashed curves just connect the points. (Data taken from Table I of reference 10 and Table IV.2 of reference 9.)

where $g_R\sim Z/A$, and

$g_s=5.585$ and $g_l=1$ for protons,

$g_s=-3.826$ and $g_l=0$ for neutrons.

Thus the calculated values of $B(E2)$ and $B(M1)$ are easily obtained once the wave functions (i.e., eigenvectors) are known.

IV. BRIEF SUMMARY OF EXPERIMENTAL REGULARITIES

The experimental regularities found in the vibrational spectra[4–8] include:

(*a*) The ratio of the energy of the second excited state to that of the first is about 2, varying from about 1.5 near the magic numbers to about 2.5 far from them. Those nuclei that have either closed neutron shell or closed proton shell have the ratio less than 2 and have the spin sequence 0^+, 2^+, 4^+, as predicted by shell-model calculations.[12] As the values of Z or N move away from the magic numbers (the value for closed shells) a second spin-two level moves close to the spin-four level and comes below the four level.[7] In this region the above ratio increases from the shell-model value of about 1.5 to a value of about 2.2 or 2.3, while the energy of the first excited state decreases. In the vibrational or near harmonic region the ratio is about 2.2, with the energy of the second 2^+ level being slightly lower than that of the 4^+ level for most cases.[5–7] As the rotational region is approached, a different trend is noted. The ratio becomes larger reaching a value of 10/3 in the rotational region, and the energy of the second 2^+ level again moves higher than the energy of the 4^+ level.[5]

(*b*) It appears that for a large number of even-even nuclei there is a strong correlation between $B(E2;2\rightarrow 0)$ and E_2 the energy of the first excited state. This correlation has been expressed as $B(E2;2\rightarrow 0)$ being proportional to $Z^2E_2^{-1.4}$ by Van Patter[7] and as F equals to

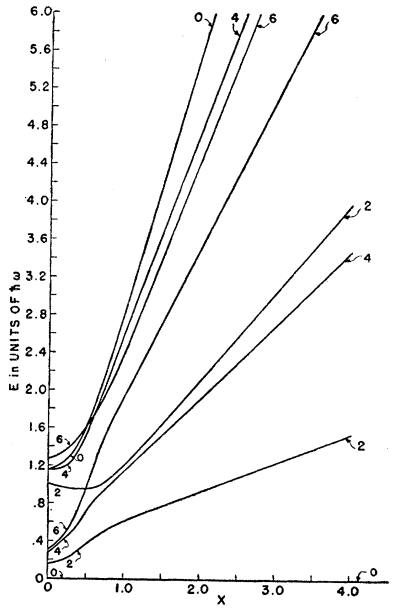

FIG. 2. The computed variation of the energy levels as a function of the deformation parameter x. The calculation is for the configuration $(7/2)^2$ and assumes $D=0.20$ and includes collective effects.

$11+320\exp(-5.1E_2)$ by Mallmann.[6] [$B(E2;2\rightarrow 0)\sim FR_0^4$.] Since the knowledge of how the parameters of the theory vary with atomic number is not known, the present calculations do not account for this systematic behavior. Attempts at obtaining these observed regularities have been unsuccessful.

A less general correlation is also observed for a fixed value of Z. In Fig. 1, the experimental values of $B(E2)/B_{SP}(E2)Z^2$ are plotted as a function of the energy, E_2, of the first excited state for those values of Z for which more than two isotopes have been measured. For these, the single-particle transition rate, $B_{SP}(E2)$, is set equal to $3e^2\times10^{-5}A^{\frac{4}{3}}\times10^{-48}$ cm^4. Since different elements presumably have different parameters associated with their deformability, each value of Z requires a separate plot. It is most encouraging to see that the general trend is the same for each value of Z. The gross features of this trend are easily understood since in moving away from a closed shell, E_2 becomes smaller and collective effects become larger, so $B(E2;2\rightarrow 0)$ increases as E_2 decreases.

(c) The $E2$ gamma-ray transitions between neighboring levels are greatly enhanced so that the crossover transition from the second excited state to the ground state is much smaller, in general, than the transition from the second to the first excited state. In addition, the ratio of $M1$ to $E2$ is often less than one in the transitions between the two levels with $I=2$.

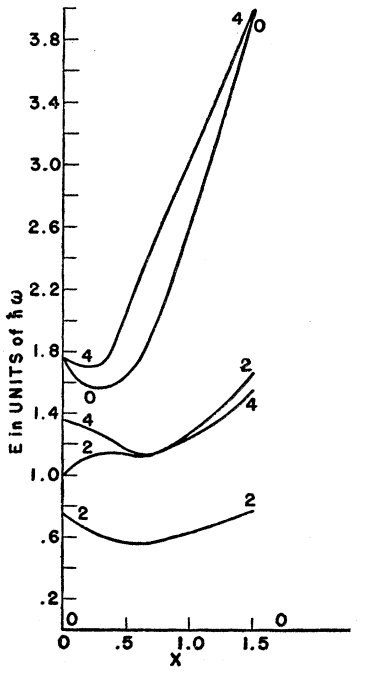

FIG. 3. The computed variation of the energy levels as a function of the deformation parameter x. The calculation is for the configuration $(7/2)^2$ and assumes $D=1.00$ and includes collective effects.

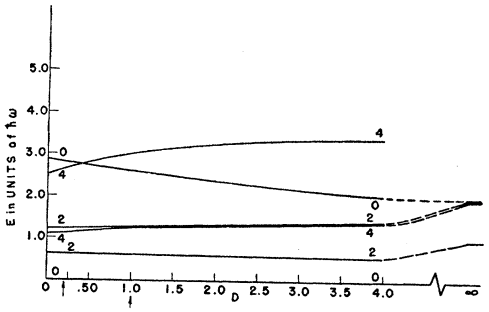

FIG. 4. The computed variation of the energy levels as a function of D, the parameter that gives the relative strength of the two-body interaction. The calculation is for the configuration $(7/2)^2$ and assumes $x=1.00$ and includes collective effects. The arrows indicate the values of D used in Figs. 2 and 3.

V. DISCUSSION OF THE THEORETICAL RESULTS

We examine first the variation of the spectrum when the strength of the two-body interaction is changed (i.e., what happens when D is varied). Two interesting features immediately emerge from the calculations. For $D\leqslant 0.4$, the energy of the first excited state increases with x and the second excited state is 4^+ for all values of x (see Fig. 2). This is easily understood by noting that the pure two-particle states lie much below the second $I=2$ state which is a one-phonon excitation of the $(\frac{7}{2})^2 J=0$ state. As D is increased, the second $I=2$ state becomes lower than the $I=4$ state and begins to repel the first $I=2$ state. Thus for $D>0.5$ the energy of the lower $I=2$ state decreases as x increases for $x\leqslant 0.7$ (see Fig. 3). As D becomes larger than 1.3 ,the states with $I=2$ exchange character, with the $I=2$ one-phonon state becoming the first excited state. This is a complex transition region, but as D approaches 4, the spectrum again becomes very simple and actually becomes very similar to a true phonon vibrational spectrum, and the second excited state has $I=4$. Here

only the $(\frac{7}{2})^2 J=0$ two-particle state is involved, since the other two-particle states are much higher in energy. The results in reference 4 would correspond to $D\sim 4$. The above comments apply only for $x\leqslant 0.7$, since as x becomes greater, the effect of D becomes negligible and the surface interaction becomes the dominant effect. This is shown in Fig. 4 where for $x=1$ the spectrum is almost independent of D. The case $D=\infty$ corresponds to a pure rotational spectrum. For all values of D, and for $x\geqslant 0.25$, the energy of the second excited state is about twice the energy of the first excited state, as observed experimentally.

To study the variation of the spectra with x, Figs. 2 and 3 are useful. In Fig. 2, D was set equal to 0.20 so that at $x=0$ the two-particle no-phonon states are well separated from the one-phonon states. As x increases, the different levels begin to mix and the spectrum becomes more complex. Note, however, in Fig. 5, that for $x\geqslant 0.25$, the energy, E_2', of the second state with

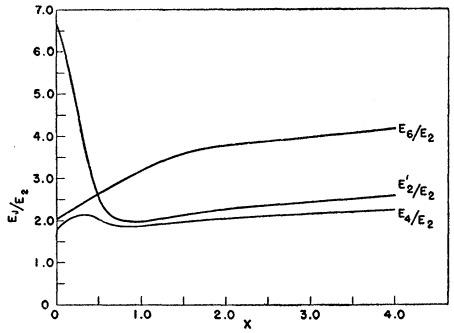

FIG. 5. The calculated ratio of the energies E_I of the excited states to the energy E_2 of the first excited state *vs* x for $D=0.20$.

$I=2$ is about double the energy, E_2, of the first state with $I=2$. This same ratio holds for E_4/E_2 for all values of x. In Fig. 3, in which D was set equal to 1.0, the spectrum is much more complicated. The second state with $I=2$ lies below the state with $I=4$ for $x<0.7$, and the energy of the first excited state decreases with increasing deformation. Upon closer examination of the spectrum for $D=1.0$ between $x=0$ and $x=0.7$, we find that it fits the experimentally observed regularities as shown in Fig. 6, where E_2'/E_2, E_4/E_2 and E_4/E_2' are plotted. This choice of $D=1$ corresponds to a not unreasonable choice of parameters. If the first excited state for $x=0$ and $D=1.0$ is put at 1.5 Mev, then $\hbar\omega$ would be equal to 2 Mev.

The variation of $B(E2;0\rightarrow 2)$ with x and D is displayed in Fig. 7. Here we note that $B(E2;0\rightarrow 2)$ is a sensitive function of x but does not vary appreciably with D. Thus $B(E2;0\rightarrow 2)$ is a good measure of the collective effects present. Note also that large values of $B(E2;0\rightarrow 2)$ may be obtained for $x\sim 0.5$, which is a rather modest deformation. The value of $B(E2;0\rightarrow 2)$ predicted for a one-phonon transition in the true vibrational picture is indicated by the arrow on the scale of Fig. 7.

FIG. 6. The variation, with x, of the calculated ratio of the energies E_I of the excited states to the energy E_2 of the first excited state, and of the ratio of E_4 to E_2', the energy of the second state with $I=2$. $D=1.00$.

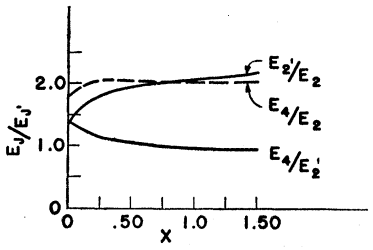

The ratios

$$B(E2;2'\rightarrow 0)/B(E2;2\rightarrow 0),$$

$$B(E20\ 2'\rightarrow 0)/B(E2;2'\rightarrow 2),$$

and

$$B(E2;2'\rightarrow 2)/B(E2;2\rightarrow 0)$$

are displayed in Figs. 8 and 9. Note in Fig. 8 how the crossover transition $2'\rightarrow 0$ rapidly decreases as x increases in agreement with the small observed experimental values. The values in Fig. 9 are to be compared with the prediction of 2.0 for the vibration model.[5]

In Fig. 10 the variation of

$$T(M1;2'\rightarrow 2)/T(E2;2'\rightarrow 2)$$

with x is displayed. This ratio is proportional to $C/\hbar\omega E_\gamma^2 Z^2 r_0^{\frac{1}{3}} A^{\frac{1}{3}}$ and Fig. 10 shows the values for a typical set of these quantities. Note the rapid decrease of the $M1$ transition with x for both neutrons and protons. This is in agreement with experimental results where E_2 is larger than $M1$ for this transition.

Figure 11 is a plot of the energy of the first excited state as a function of $B(E2;0\rightarrow 2)/Z^2 B_{\mathrm{SM}}(E2)$ for $D=1.0$ and $x<0.7$. This curve agrees qualitatively with the experimental results displayed in Fig. 1.

Th us for $D=1.0$, the systematic experimental features are obtained theoretically. In Tables II and

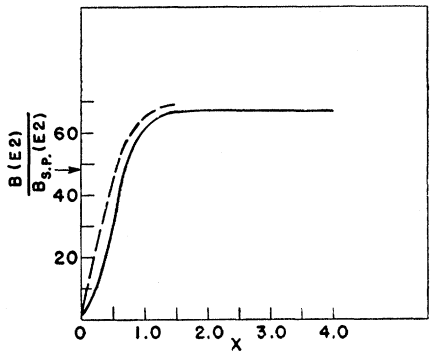

FIG. 7. Calculated curve of $B(E2)/B_{\mathrm{SM}}(E2)$ *vs* x for the transition $0^+\rightarrow 2^+$. The reduced transition probability $B(E2)$ is computed on the assumption that $Z=20$ and $(\hbar\omega/C)=0.10$, and $B_{\mathrm{SM}}(E2)$ is the shell-model value for the transition $0^+\rightarrow 2^+$. The solid curve is for $D=0.20$; the dotted curve is for $D=1.00$. The arrow indicates the value of $B(E2)/B_{\mathrm{SM}}(E2)$ for a pure one-phonon transition. [For this transition, $B_{\mathrm{SM}}(E2)$ is about equal to $B_{\mathrm{SP}}(E2)$.]

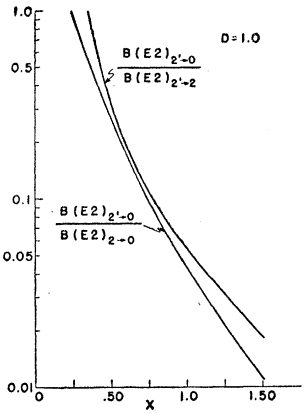

FIG. 8. The calculated ratios of (a) $B(E2; 2' \rightarrow 0)$ to $B(E2; 2 \rightarrow 0)$, and (b) $B(E2; 2' \rightarrow 0)$ to $B(E2; 2' \rightarrow 2)$ as a function of the deformation parameter x, for $D=1.00$.

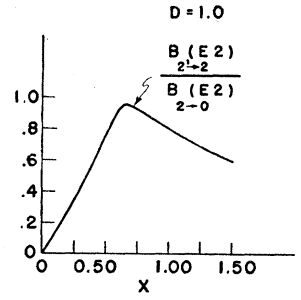

FIG. 9. The calculated ratio of $B(E2; 2' \rightarrow 2)$ to to $B(E2; 2 \rightarrow 0)$ as a function of the deformation parameter x, for $D=1.00$. The pure vibrational model gives a value of 2 for this quantity.[5]

III, the eigenfunction of the lowest level with $I=0$ is tabulated for various values of D and x. The complex nature of this eigenfunction can be clearly seen. As x increases, the states with 2 and even 3 phonons become important; but as D increases, the opposite effect takes place for this state. As D tends to infinity, the amplitudes of the phonon-excitation states go toward zero. Thus this ground state forms the base level of a true vibrational spectrum.

For the eigenfunction with $I=2$, the behavior is more complicated since the lowest two levels mix very strongly as D approaches 1.3, and the lower level has more one-phonon states in it. This is the cause of the increase in $B(E2; 0 \rightarrow 2)$ in Fig. 7 as D goes from 0.20 to 1.0.

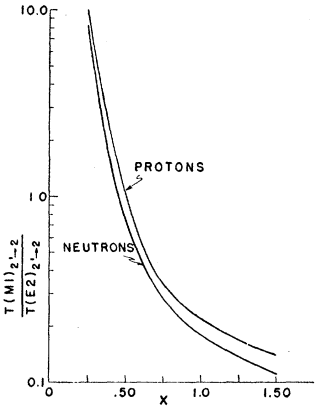

FIG. 10. The calculated ratios of the γ-ray transition probabilities $T(M1; 2' \rightarrow 2)$ to $T(E2; 2' \rightarrow 2)$ for two neutrons and for two protons as a function of the deformation parameter x, for $D=1.00$. This quantity $T(M1; 2' \rightarrow 2)/T(E2; 2' \rightarrow 2)$ is proportional to $(C/\hbar\omega E_\gamma^2 Z^2 r_0^{4/3} A^{4/3})$ and for this graph the following values are used: $\hbar\omega=0.10C$, $E_\gamma=1$ Mev, $Z=30$, $r_0=1.41\times10^{-13}$ cm, $A=66$, and also the collective g factor $g_R=\frac{1}{2}$.

Now the validity of these calculations must be examined. The neglecting of configuration interaction is justified by results[12,13] around $A=40$ and by the assumption that collective effects include some of the effects due to configuration interaction. The validity of the cutoff at three phonons is thus the only other main point to be discussed. Figure 12 shows the effect of including four phonons in the calculation. The difference is less than 10% for the lowest eigenvalues for $x<2.0$; therefore, since the main region of interest is for $x \leqslant 0.7$ our results should be quite adequate. Note, however, that the calculation of the second lowest level is not nearly as accurate and deviates appreciably from the four-phonon solution. This makes the energy of the second 0^+ level at $x=0.5$ for the three-phonon solution 14% higher than for the four-phonon solution. The same type of effect should be taken into account for levels with $I=2^+$, and thus any correction would bring the second 2^+ level down compared to the lowest 4^+ level, and thus tend to improve the agreement with experiment. Unfortunately, the four-phonon solution

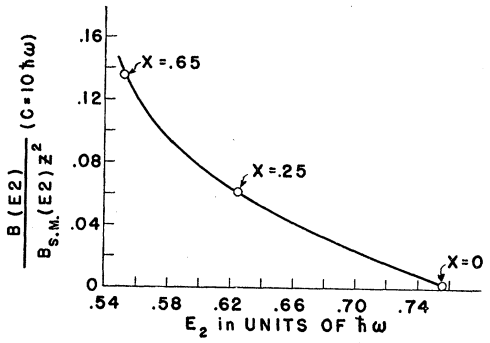

FIG. 11. Calculated values of $B(E2; 0 \rightarrow 2)/Z^2 B_{SM}(E2)$, assuming $C=10\hbar\omega$, p otted as a function of E_2, for $D=1.00$ and $0 \leqslant x \leqslant 0.7$. This is to be compared with the experimental values in Fig. 1 since there $B_{SM}(E2) \cong B_{SP}(E2)$.

for $I=2$ involves diagonalizing a 40×40 matrix and does not seem to be a profitable undertaking at present.

In summary, the theoretical results show that

(*a*) for $x>0.25$ and all values of D, the second 2^+ state and the lowest 4^+ state are at about twice the energy of the first excited state;

(*b*) for $D \leqslant 0.4$, the energy of the first excited state increases with x and the second excited state has spin 4^+ for all values of x;

(*c*) for $D>0.4$, the energy of the first excited state decreases as x increases, and when $D=1.0$ the energy of the second 2^+ level is lower than that of the 4^+ level for $x<0.7$;

(*d*) for $x>1.0$, the spectrum becomes almost independent of D;

(*e*) the transition probability, $B(E2; 0 \rightarrow 2)$, is a rapidly increasing function of x even for small x and does not depend sensitively on D;

(*f*) for $D=1.0$, and $x<0.7$, the calculated variation

of $B(E2;0\rightarrow 2)$ with E_2 is similar to the observed variation for a given value of Z;

(g) for $D=1.0$ and $x>0.35$, the observed selection rules involving γ-ray transitions can be obtained, namely, the direct transitions are favored over the crossover transition, and $T(M1)/T(E2)$ is less than one for the $2'\rightarrow 2$ transition.

VI. CONCLUSIONS

The observed regularities in even-even nuclei in the "vibrational" region can be explained by combining interparticle and collective interactions. The general features of vibrational spectra are also found for situations far removed from the vibrational picture assumed by Scharff-Goldhaber and Weneser.[4] Indeed the best fit to the observed regularities occurs in the region of true intermediate coupling where both interparticle and collection interactions are important.

These calculations agree quite well with the observed level spacing and γ-ray transition rates. The spin of the second excited state is 2^+, with a 4^+ state at slightly higher energy, as often observed experimentally. The recent measurement[19] of an $E0$ transition in competition with $M1$ and $E2$ has made this quantity of theoretical interest. Further calculations are in progress to determine the theoretical values of the $E0$ transition probability.

The pure vibrational picture is thus not necessary to explain even-even nuclei. A better fit to the observed regularities is obtained when interparticle forces are included with the collective effects.

These conclusions are based on the assumption that choosing different shell-model states would not appreciably change the theoretical results. This assumption has been explored in the limit of no interparticle forces and weak surface coupling by Ford and Levinson.[11] Their results indicate that for even-even nuclei, the general behavior does not change with shell-model configuration. This is also qualitatively true for interparticle forces.[20] Thus it seems reasonable to apply these results beyond the $f_{\frac{7}{2}}$ shell, keeping in mind that in that region the agreement is qualitative and that for detailed quantitative results other similar calculations must be performed for other shell-model configurations.

TABLE II. Eigenvalues in units of $\hbar\omega$ and wave functions for the lowest $I=0$ level for $D=1.00$ and various values of x, the deformation parameter.

$J\ R\ P$ \ x / $-\lambda$	0 2.2982	0.25 2.5336	0.65 3.7618	1.0 5.2817	1.5 7.6542
0 0 0	1.000	0.9345	0.6818	0.5355	0.4394
2 2 1		−0.3408	−0.5946	−0.6118	−0.6077
0 0 2		0.0689	0.2694	0.3470	0.3840
2 2 2		−0.0468	−0.1889	−0.2514	−0.2867
4 4 2		0.0542	0.2089	0.2744	0.3120
0 0 3		0.0072	0.0550	0.0840	0.1029
2 2 3		−0.0195	−0.1520	−0.2353	−0.2917
4 4 3		0.0054	0.0445	0.0722	0.0934
6 6 3		−0.0046	−0.0367	−0.0592	−0.0767

TABLE III. Eigenvalues in units of $\hbar\omega$ and wave functions for the lowest $I=0$ level for $x=1.00$ and various values of D, the parameter that measures the relative strength of the two-body interaction.

$J\ R\ P$ \ D / $-\lambda$	0 3.5195	0.20 3.8649	0.65 4.6550	1.0 5.2817	2.0 7.1278	4.0 11.0409
0 0 0	0.4681	0.4816	0.5120	−0.5355	0.6015	0.7191
2 2 1	−0.6381	−0.6351	−0.6268	−0.6188	−0.5897	−0.5147
0 0 2	0.3250	0.3300	0.3402	0.3470	0.3605	0.3606
2 2 2	−0.2744	−0.2704	−0.2602	−0.2514	−0.2232	−0.1645
4 4 2	0.3318	0.3197	0.2936	0.2744	0.2250	0.1492
0 0 3	0.0841	0.0844	0.0844	0.0840	0.0807	0.0678
2 2 3	−0.2461	−0.2444	−0.2397	−0.2353	−0.2195	−0.1791
4 4 3	0.0894	0.0859	0.0781	0.0722	0.0568	0.0334
6 6 3	−0.0825	−0.0772	−0.0665	−0.0592	−0.0424	−0.0220

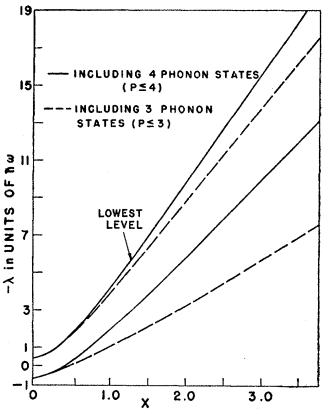

FIG. 12. The two lowest eigenvalues for $I=0$ plotted as functions of x, the deformation parameter, assuming $D=0.20$. The solid curves include not more than 4 phonons of excitation, the broken curves include not more than 3 phonons of excitation. Note that the scale has been inverted so that the upper curves are the lowest eigenvalues.

VII. ACKNOWLEDGMENTS

The author wishes to thank J. B. French for suggesting this research and for interest, assistance, and encouragement during the initial stages of this work. The author is indebted to D. Kurath for many enlightening discussions and valuable criticisms, and for aid in formulating the problem for machine computation. He also wishes to thank C. A. Mallmann and D. M. Van Patter for valuable discussions and correspondence, and J. Weneser and G. Scharff-Goldhaber for their critical reading of the manuscript from which valuable insight was gained. The Applied Mathematics Division of Argonne National Laboratory, especially J. A. Nelson and B. Garbow, were of great assistance.

[19] T. R. Gerholm and B. G. Pettersson, Phys. Rev. **110**, 1119 (1958).

[20] M. G. Mayer and J. H. D. Jensen, *Elementary Theory of Nuclear Structure* (John Wiley & Sons, Inc., New York, 1955).